Metasomatized lithospheric mantle for Mesozoic giant gold deposits in the North China craton

Zaicong Wang[1]*, Huai Cheng[1], Keqing Zong[1], Xianlei Geng[1], Yongsheng Liu[1], Jinhui Yang[2], Fuyuan Wu[2], Harry Becker[3], Stephen Foley[4] and Christina Yan Wang[5]

[1]State Key Laboratory of Geological Processes and Mineral Resources (GPMR), School of Earth Sciences, China University of Geosciences, Wuhan 430074, China
[2]Institute of Geology and Geophysics, Chinese Academy of Sciences, Beijing 100029, China
[3]Institut für Geologische Wissenschaften, Freie Universität Berlin, Berlin 12249, Germany
[4]Department of Earth and Environmental Sciences, Macquarie University, North Ryde, NSW 2109, Australia
[5]Guangzhou Institute of Geochemistry, Chinese Academy of Sciences, Guangzhou 510640, China

ABSTRACT

The origin of giant lode gold deposits of Mesozoic age in the North China craton (NCC) is enigmatic because high-grade metamorphic ancient crust would be highly depleted in gold. Instead, lithospheric mantle beneath the crust is the likely source of the gold, which may have been anomalously enriched by metasomatic processes. However, the role of gold enrichment and metasomatism in the lithospheric mantle remains unclear. Here, we present comprehensive data on gold and platinum group element contents of mantle xenoliths ($n = 28$) and basalts ($n = 47$) representing the temporal evolution of the eastern NCC. The results indicate that extensive mantle metasomatism and hydration introduced some gold (<1–2 ppb) but did not lead to a gold-enriched mantle. However, volatile-rich basalts formed mainly from the metasomatized lithospheric mantle display noticeably elevated gold contents as compared to those from the asthenosphere. Combined with the significant inheritance of mantle-derived volatiles in auriferous fluids of ore bodies, the new data reveal that the mechanism for the formation of the lode gold deposits was related to the volatile-rich components that accumulated during metasomatism and facilitated the release of gold during extensional craton destruction and mantle melting. Gold-bearing, hydrous magmas ascended rapidly along translithospheric fault zones and evolved auriferous fluids to form the giant deposits in the crust.

INTRODUCTION

The subcratonic lithospheric mantle (SCLM) underneath Archean crust mostly formed by high degrees of partial melting (Griffin et al., 2009). The SCLM is thus refractory and strongly depleted in incompatible elements and many metals like Au, reducing its potential as a source for later giant deposits. However, magmas and fluids derived from the convecting mantle, and particularly subducted materials, may have metasomatized and replenished the SCLM in volatiles, metals, and other elements (e.g., Lorand et al., 2013; O'Reilly and Griffin, 2013). The metasomatized SCLM is often assumed to be anomalously enriched in Au and to represent the source for the formation of large Au provinces (Hronsky et al., 2012; Griffin et al., 2013;

Tassara et al., 2017), including Carlin-type Au deposits (sediment-hosted disseminated gold deposits) (Muntean et al., 2011).

Giant Au deposits in the North China craton (NCC), which are globally noteworthy for their large-scale reserves (>5000 tons), are likely the best case in the world to clarify this model. The lithospheric mantle of the NCC was intensely metasomatized and hydrated over 2 billion years by partial melts and subducted components of different ages (Paleozoic, Triassic, Jurassic) before its extensive destruction at ca. 130–120 Ma (Zhu et al., 2012; Wu et al., 2019). The cratonic destruction was essentially coeval with the eruption of mantle-derived magmas and the formation of giant lode Au deposits in the eastern NCC (Li et al., 2012; Zhu et al., 2015). These hydrothermal deposits are mostly hosted in amphibolite- to granulite-facies metamorphic rocks and in Mesozoic felsic plutons. They are difficult

to designate as crustal metamorphism-related orogenic Au deposits because they formed prior to 1.8 Ga after high-grade metamorphism of the crust, which would have been strongly depleted in gold and fluids (Goldfarb and Santosh, 2014; Goldfarb and Groves, 2015). Instead, it is assumed that the lithospheric mantle of the NCC metasomatized by subducted materials may have played a key role in the large-scale Au mineralization (Goldfarb and Groves, 2015; Li et al., 2012; Zhu et al., 2015).

However, the extent of gold enrichment in the SCLM after metasomatism and the mechanism and scope of its contribution to giant Au deposits have rarely been directly tested. Here, we present Au and platinum group element (PGE) contents of the peridotite xenoliths and basalts in the NCC, which reflect different evolutionary episodes of the mantle from the Archean to Cenozoic. This allows us to fully assess the impact of metasomatism on the Au contents of the SCLM and define the links among mantle metasomatism, mantle-derived hydrous magmas, and the origin of giant Au deposits in the NCC.

SAMPLES

Primitive alkaline picrites and high-Mg basalts with Mg# of 71–75 were erupted coeval with (125–119 Ma) (Fig. 1), or slightly earlier than the peak period of Au mineralization (Gao et al., 2008; Liu et al., 2008). They have been extensively studied and are characterized by high volatile contents (e.g., 2–4 wt% water), arc basalt–like trace element patterns, and radiogenic Sr-Nd-Hf-Os isotopic compositions (referred to hereafter as 130–120 Ma basalts; Zhang et al., 2002; Gao et al., 2008; Liu et al., 2008; Xia et al., 2013; Meng et al.,
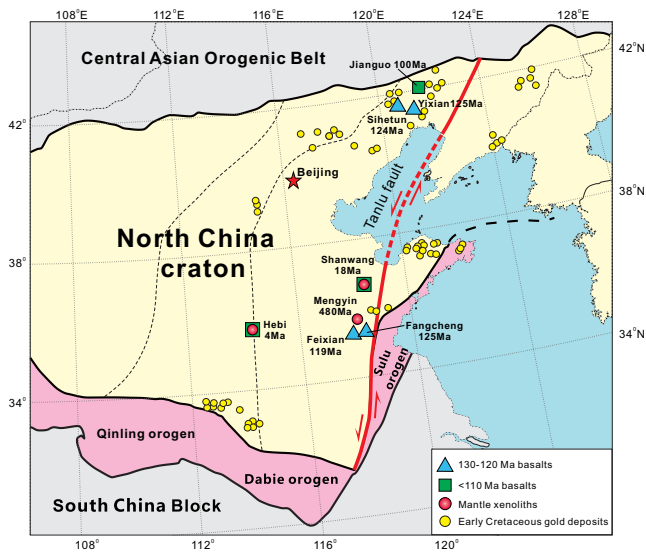
*E-mail: zaicongwang@cug.edu.cn

Figure 1. Sample locations on a simplified map of the North China craton (NCC). Analyzed mantle xenoliths and basalts (130–120 Ma and <110 Ma) are shown with eruption ages. Both mantle xenoliths and basalts from Hebi and Shanwang are included. Also shown are the major districts of Early Cretaceous lode gold deposits and the trans-lithospheric Tanlu fault in the eastern North China craton (modified from Zhu et al., 2015).

2015; Huang et al., 2017; Geng et al., 2019a, 2019b). They have been well accepted to have mainly originated from metasomatized, hydrated and isotopically enriched SCLM with insignificant input of crustal contamination (see details in the GSA Data Repository[1]). We analyzed the Au and PGE contents of many 130–120 Ma basalts, and younger basalts that erupted after the formation of the gold deposits. The younger basalts erupted later than 110 Ma and are melts derived from the asthenosphere (Liu et al., 2008; Meng et al., 2015). We used these basalts as a measure for the fraction of gold released from the asthenospheric mantle compared to the 130–120 Ma basalts, which were mainly from the metasomatized SCLM. Mantle xenoliths with Archean to Paleoproterozoic (Hebi and Mengyin) and Phanerozoic (Shanwang) Re depletion model ages (Zheng et al., 2005; Chu et al., 2009; Liu et al., 2011) were also analyzed to assess temporal changes in the Au contents of the SCLM.

We obtained the gold and PGE contents of bulk rocks of mantle xenoliths (*n* = 28, three locations; Fig. 1), and 130–120 Ma and <110 Ma basalts (*n* = 47, seven locations), after Carius tube digestion in reverse aqua regia and chromatography separation (Cheng et al., 2019). The PGE contents were determined by isotope dilution methods, and gold contents were determined by internal standardization to platinum and/or standard addition method (Tables DR1–DR2 in the Data Repository). Reference materials and sample replicates indicated 10%–15% (2 standard deviations) uncertainty for Au, with blanks of 5 ± 5 pg

(Figs. DR1–DR3). Such low blanks are essential for analyzing low-Au samples. The Au and PGE contents and other information about the analyzed samples are given in Tables DR1–DR3, and the main results are shown in Figures 2 and 3.

LIMITED RE-ENRICHMENT OF GOLD IN METASOMATIZED MANTLE

Gold is more incompatible, and also more mobile, in fluids than Pd and other PGEs (Maier et al., 2012; Pokrovski et al., 2013), and so melt and/or fluid metasomatism should elevate the Au/Ir and Pd/Ir ratios of the refractory SCLM, and also Au/Pd, which is a well-documented feature of peridotites (e.g., Fischer-Gödde et al., 2011; Maier et al., 2012). The Mengyin mantle xenoliths hosted by 480 Ma kimberlites, and the Hebi mantle xenoliths hosted by 4 Ma basalts, represent the relics of Archean–Paleoproterozoic SCLM (low $^{187}Os/^{188}Os_{initial}$ of 0.1089–0.1164, high Mg# of > 92; Fig. 2). They have undergone extensive metasomatism, as indicated by highly enriched light rare earth elements (REEs; Zheng et al., 2005), radiogenic $^{87}Sr/^{86}Sr_{initial}$, and unradiogenic $^{143}Nd/^{144}Nd_{initial}$ (Zhang et al., 2008; Chu et al., 2009). The Mengyin harzburgite xenoliths contain 140–510 ppm S, which is much higher than that for refractory peridotites (Chu et al., 2009), and variably elevated Au/Pd$_{(N)}$ (normalized to the primitive mantle [PM]), indicating the addition of sulfides and gold during metasomatism. However, these samples still contain relatively low Au contents of 0.06–0.50 ppb, as well as low Pd and Cu contents compared to the PM (Fig. 2). This is also true for the Hebi peridotites (La/Yb$_{(N)}$ of 16–38 and Au of 0.03–0.11 ppb; Fig. 2). These results indicate that metasomatism introduced S, but only limited Au, into the SCLM from the Archean to 480 Ma, and even until 4 Ma in the central NCC (Hebi). A similar fashion of Au enrichment also occurred in the Finsch and

Venetia peridotites in the Kaapvaal craton (e.g., high S contents of 280–1240 ppm and high Au/Pd$_{(N)}$ of >1–13, but Au <0.9–1.4 ppb; Maier et al., 2012). The Shanwang peridotite xenoliths hosted in 18 Ma basalts represent juvenile lithospheric mantle that formed after the destruction of the NCC and Mesozoic Au mineralization (Chu et al., 2009). They contain 0.02–1.8 ppb Au and show a correlation with PGE contents, similar to refertilized massif-type peridotites representative of Phanerozoic lithospheric mantle (Figs. 2 and 3; Fig. DR4).
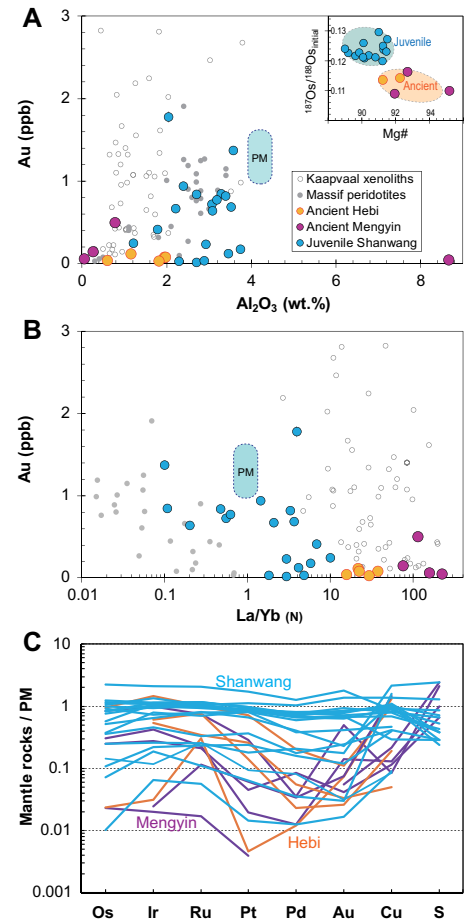

Figure 2. (A–C) Gold and platinum group element (PGE) contents of mantle xenoliths in the North China craton (NCC). Xenoliths in the Hebi and Mengyin areas (A–B) represent relics of Archean to Paleoproterozoic refractory subcratonic lithospheric mantle (SCLM) with later strong metasomatism (Chu et al., 2009; Liu et al., 2011); Shanwang xenoliths are from juvenile SCLM after the destruction of NCC lithosphere (Chu et al., 2009). For many peridotite xenoliths from the Kaapvaal craton, South Africa (Maier et al., 2012), metasomatism contributed abundant sulfur and other volatiles but limited Pd, Au, and Cu to SCLM (C). Data for re-fertilized massif-type peridotites from the Ivrea zone (Italian Alps; Wang et al., 2013) are shown for comparison. Primitive mantle (PM) normalization values are from the literature (McDonough and Sun, 1995; Becker et al., 2006).
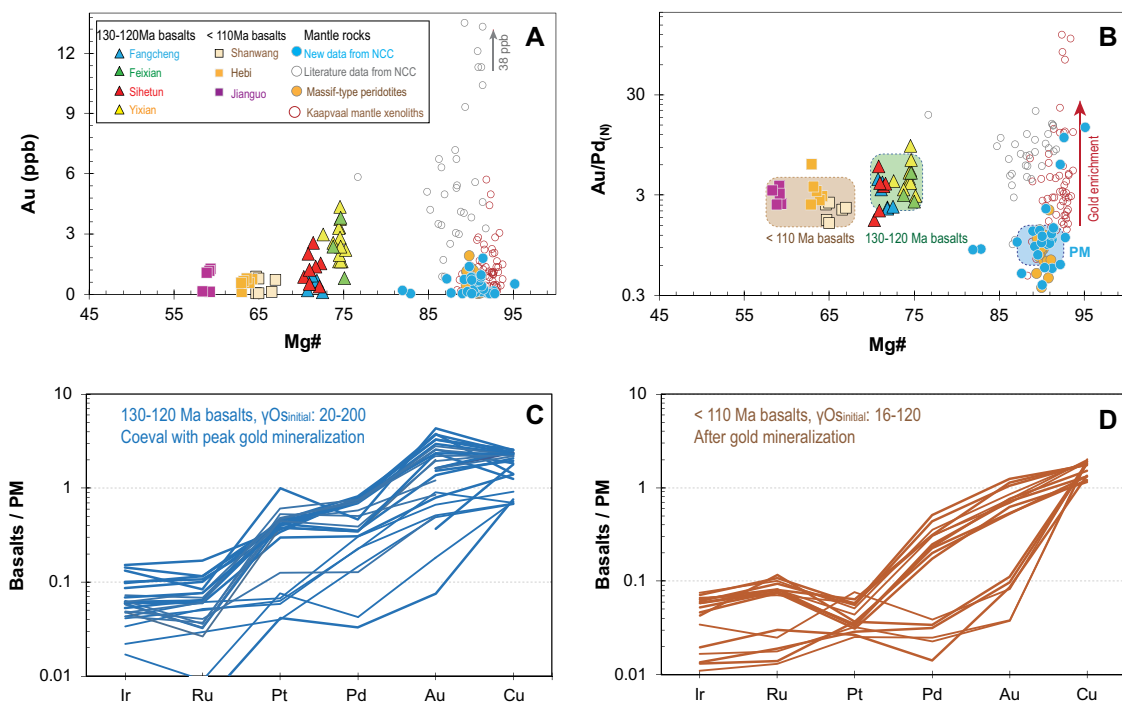
Figure 3. (A–D) Gold and platinum group element (PGE) contents of 130–120 Ma and <110 Ma basalts in the North China craton, showing that 130–120 Ma basalts have generally high Au contents but only slightly elevated Au/Pd$_{(N)}$ relative to <110 Ma basalts and mantle xenoliths (A,B). Note that new data from mantle xenoliths are comparable to re-fertilized massif-type peridotites (Wang et al., 2013), but show far lower gold contents than previous values of mantle rocks in the North China craton (NCC; Zheng et al., 2005; Zhang et al., 2008). Overall, 130–120 Ma basalts contain enhanced Au, Ir, and Pt contents relative to <110 Ma basalts (C,D). Radiogenic Os isotopes of 130–120 Ma basalts suggest selective and efficient release of metals from the fusible fraction of metasomatized SCLM. Strongly metasomatized Kaapvaal (South Africa) peridotite xenoliths (Maier et al., 2012) are shown for comparison. PM—primitive mantle.

Previously determined Au contents of mantle xenoliths from the NCC, mainly by the NiS fire assay method, showed a large range of 0.5–38 ppb, with a mean value of 5 ppb; this is distinctly different from other mantle domains worldwide, including those with strong mantle metasomatism (Fischer-Gödde et al., 2011; Saunders et al., 2018). Our high-precision new Au data are far lower than the previous values (Figs. 2 and 3; Fig. DR5), including those from the same localities (3–13 ppb Au; Zhang et al., 2008; Zheng et al., 2005). Such discrepancy likely does not result from sample heterogeneity but data quality (see the Data Repository). The new data are consistent with Cu and PGE contents in the same samples as well as other peridotites of variable fertility worldwide (Fig. 2; see the Data Repository). Therefore, the mantle xenoliths, reflecting metasomatized ancient SCLM and juvenile SCLM beneath the NCC, indicate no substantial enrichment of Au, Cu, or Pd contents. The NCC is thus unlikely to have been inherently rich in Au, and mantle metasomatism and replacement by juvenile lithospheric mantle may not have led to strong enrichment of Au in the SCLM.

The 130–120 Ma basalts from the northern and southern margins of the NCC contain a mean value of 2.2 ppb Au, with a maximum of 4.3 ppb (0.4–4.3 ppb Au, $n = 24$; Figs. 3 and 4). Despite the much longer history of metasomatism, the 130–120 Ma basalts mostly display Au/Pd$_{(N)}$ of 3–5, i.e., only slightly higher than those for the <110 Ma basalts (2–4) and the fertile mantle (0.5–2). The Au contents and Au/Pd$_{(N)}$ of the 130–120 Ma basalts thus reflect limited enrichment of Au relative to PGEs and the low Au contents of the lithosphere beneath the eastern NCC (Fig. 3). This observation is remarkable because the northern and southern cratonic margins of the NCC were considered to have been strongly affected by multiple periods of subduction from 480 Ma to 130 Ma (Zhu et al., 2012; Wu et al., 2019) and to be essential for the Au deposits (Goldfarb and Groves, 2015; Zhu et al., 2015). All of the new data for the mantle xenoliths and basalts of the eastern NCC consistently indicate that there is no significant Au enrichment in the SCLM, despite extensive metasomatism and hydration. Mantle metasomatism and hydration did replenish a fraction of Au to the highly depleted SCLM, as reflected by the elevated Au/Pd$_{(N)}$, but the amount must have been limited (Figs. 2 and 3).

EFFICIENT RELEASE OF GOLD INTO HYDROUS BASALTS

Although the metasomatized SCLM does not show anomalous enrichment of Au, the hydrous 130–120 Ma basalts derived from the SCLM contain 2–3 ppb Au on average, which is 3–4 times higher than values of asthenosphere-derived, <110 Ma basalts (Figs. 3 and 4). This is remarkable given similarly low Au contents (<1–2 ppb) of the mantle source as indicated by similar Au/Pd$_{(N)}$ (Figs. 3 and 4). Metasomatism led to high H$_2$O contents (>1000 ppm), S, C, and other volatiles, and elevated oxygen fugacity in the SCLM beneath the NCC (Geng et al., 2019a, 2019b; Xia et al., 2013). The 130–120 Ma basalts contain high MgO of 11–14 wt% and high water contents, which resulted from high degrees of partial melting of the metasomatized SCLM. Increasing H$_2$O contents and oxygen fugacity of the basalts from the metasomatized source could lead to a preferential transfer of Au into the magma (Botcharnikov et al., 2011). These basalts show enhanced Au and PGE contents (e.g., 0.1–0.5 ppb Os-Ir), and particularly radiogenic ^{187}Os/^{188}Os$_{initial}$ values (Gao et al., 2008; Huang et al., 2017). These data support the selective and efficient release of metals from the fusible fraction of the metasomatized SCLM, irrespective of the specific rock types, including the possible gold-rich veins in metasomatized peridotites (Tassara et al., 2017). High-degree hydrous melting thus promoted the release of the fusible components of the SCLM with Au into 130–120 Ma basalts. In contrast, after the NCC destruction, the juvenile lithospheric and asthenospheric mantle was relatively volatile-poor (Zhu et al., 2012; Xia et al., 2017), and so <110 Ma basalts have low Au and PGE contents, like mid-ocean-ridge basalts (Figs. 3 and 4).

We conclude that the relatively high Au contents of the 130–120 Ma, volatile-rich basalts mainly resulted from efficient extraction from metasomatized SCLM. A similar process likely also occurred for the giant Lihir gold deposit in Papua New Guinea, where the adjacent mantle source was strongly modified by subduction but metal contents remained low, e.g., only 0.04–1.29 ppb Au and 9–40 ppm Cu (McInnes et al., 1999), comparable to the metasomatized SCLM of the NCC.
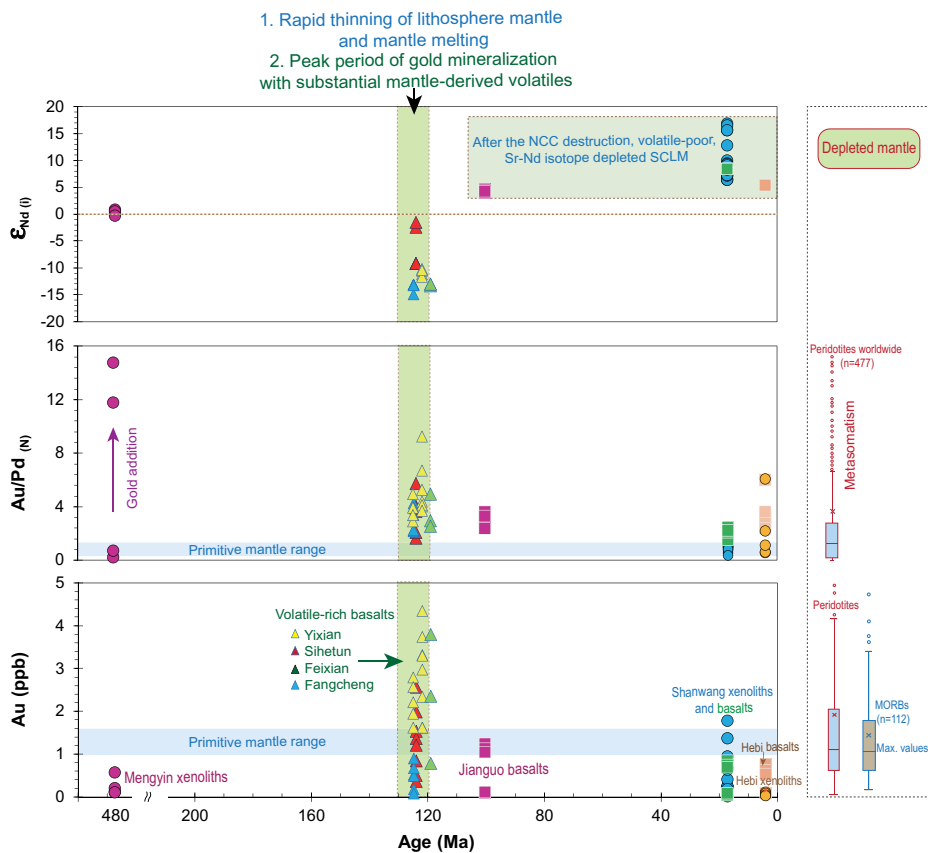
Figure 4. Temporal evolution of the North China craton (NCC) lithosphere and its relation to Mesozoic giant gold deposits. Before 480 Ma, refractory Archean subcratonic lithospheric mantle (SCLM) was metasomatized over 1.8 b.y. by volatile-rich melts/fluids (Chu et al., 2009), adding a limited amount of gold, as reflected by the Mengyin and Hebi xenoliths. Multiple subduction episodes between the Paleozoic and Mesozoic further strongly metasomatized and hydrated the SCLM (Wu et al., 2019). 130–120 Ma basalts mainly originated from extension-driven, high-degree melting of metasomatized SCLM, and sampled the most fusible components from a large volume of the mantle source. They were hydrous, volatile-rich, and gold-bearing components, and contributed fluids and gold for giant lode gold deposits, which inherited mantle volatiles (Mao et al., 2008; Zhu et al., 2015; Tan et al., 2018). Basalts that erupted after NCC lithosphere destruction (Jianguo, Shanwang, and Hebi) and juvenile SCLM (Shanwang) display generally low Au contents. Peridotites worldwide (Saunders et al., 2018) and mid-ocean-ridge basalts (MORBs; Jenner and O'Neill, 2012) are shown for comparison. Note that MORB data should represent maximum values because many basalts show contents lower than the detection limit (Jenner and O'Neill, 2012).

IMPLICATIONS FOR GIANT GOLD DEPOSITS IN THE NCC

The 130–120 Ma basalts in the NCC provide key insights into the links in timing and mechanism among the metasomatized SCLM, hydrous mantle magmas, and ore-forming fluids that record a strong signature of mantle-derived volatiles (Fig. 4). The extension-induced thinning of the SCLM beneath the NCC and its conversion into juvenile lithosphere by upwelling asthenospheric mantle at ca. 130–120 Ma (Zhu et al., 2012; Wu et al., 2019) triggered the high degree of melting of the metasomatized SCLM. This resulted in the formation of hydrous S-, C-, Cl-, and Au-bearing, high Mg# magmas, as reflected by the 130–120 Ma basalts that erupted almost coeval with the peak of gold mineralization. The rapid ascent and emplacement of the magmas along pre-existing lithosphere-scale weak zones such as the

Tanlu fault (Zhao et al., 2016) were facilitated by the preconcentration of hydrous mineral assemblages in these weak zones (Foley, 2008).

With further magmatic-hydrothermal evolution, the gold that was initially in the hydrous magmas would have favorably partitioned into the exsolved fluids and would have been significantly enriched in the fluids by a factor of hundreds (Pokrovski et al., 2013). The fluids then preferentially transported Au, S, Cl, C, and noble gases along the translithospheric faults to second-order fault systems, where Au was deposited. This model explains the strong spatial and temporal association of Au deposits with metasomatized lithospheric sources of mafic dike swarms, the major association between Au deposits and extensional fault systems (Goldfarb and Santosh, 2014), and the substantial inheritance of mantle-derived volatile S, C, H, O

(Mao et al., 2008) and noble gases (Zhu et al., 2015; Tan et al., 2018) in the auriferous fluids of ore bodies. Primitive basaltic magmas with 2–3 ppb Au, similar to those of the parental magmas (1.5–4 ppb Au) of the giant Bingham Canyon (Utah, USA) Cu-Au porphyry deposit (Grondahl and Zajacz, 2017), could have led to the formation of giant Au deposits such as those observed in the eastern NCC.

Consequently, significant Au pre-enrichment in the SCLM is not a prerequisite for the formation of giant Au deposits. Extensive mantle metasomatism plays a key role in that it enables the efficient extraction of Au during subsequent melting of the metasomatized mantle. The metasomatic components are probably also essential to produce later auriferous fluids that are exsolved and lead to the giant Au deposits. The present work highlights the importance of mantle-derived, Au-bearing hydrous magmas in the origin of giant Au deposits. Further understanding of the detailed magmatic-hydrothermal evolution is required for a complete picture of the enrichment stages of Au.

REFERENCES CITED
Becker, H., Horan, M.F., Walker, R.J., Gao, S., Lorand, J.-P., and Rudnick, R.L., 2006, Highly siderophile element composition of Earth's primitive upper mantle: Constraints from new data on peridotite massifs and xenoliths: Geochimica et Cosmochimica Acta, v. 70, p. 4528–4550, https://doi .org/10.1016/j.gca.2006.06.004.

Botcharnikov, R.E., Linnen, R.L., Wilke, M., Holtz, F., Jugo, P.J., and Berndt, J., 2011, High gold concentrations in sulphide-bearing magma under oxidizing conditions: Nature Geoscience, v. 4, p. 112–115, https://doi.org/10.1038/ngeo1042.

Cheng, K., Wang, Z., Chen, K., Zong, K., Zou, Z., He, T., Hu, Z., Fischer-Gödde, M., and Liu, Y., 2019, High-precision determination of gold mass fractions in geological reference materials by internal standardisation: Geostandards and Geoanalytical Research, https://doi.org/10.1111/ggr.12284.

Chu, Z.Y., Wu, F.Y., Walker, R.J., Rudnick, R.L., Pitcher, L., Puchtel, I.S., Yang, Y.H., and Wilde, S.A., 2009, Temporal evolution of the lithospheric mantle beneath the eastern North China craton: Journal of Petrology, v. 50, p. 1857–1898, https:// doi.org/10.1093/petrology/egp055.

Fischer-Gödde, M., Becker, H., and Wombacher, F., 2011, Rhodium, gold and other highly siderophile elements in orogenic peridotites and peridotite xenoliths: Chemical Geology, v. 280, p. 365–383, https://doi.org/10.1016/j.chemgeo.2010.11.024.

Foley, S.F., 2008, Rejuvenation and erosion of the cratonic lithosphere: Nature Geoscience, v. 1, p. 503, https://doi.org/10.1038/ngeo261.

Gao, S., Rudnick, R.L., Xu, W.-L., Yuan, H.-L., Liu, Y.-S., Walker, R.J., Puchtel, I.S., Liu, X., Huang, H., Wang, X.-R., and Yang, J., 2008, Recycling deep cratonic lithosphere and generation of intraplate magmatism in the North China craton: Earth and Planetary Science Letters, v. 270, p. 41–53, https://doi.org/10.1016/j.epsl.2008.03.008.

Geng, X., Foley, S.F., Liu, Y., Wang, Z., Hu, Z., and Zhou, L., 2019a, Thermal-chemical conditions of the North China Mesozoic lithospheric mantle and implication for the lithospheric thinning of cratons: Earth and Planetary Science Letters, v. 516, p. 1–11, https://doi.org/10.1016/j.epsl.2019.03.012.

Geng, X., Liu, Y., Wang, X.-C., Hu, Z., Zhou, L., and Gao, S., 2019b, The role of Earth's deep volatile cycling in the generation of intracontinental high-Mg andesites: Implication for lithospheric thinning beneath the North China craton: Journal of Geophysical Research–Solid Earth, v. 124, p. 1305–1323, http://doi:10.1029/2018JB016157.

Goldfarb, R.J., and Groves, D.I., 2015, Orogenic gold: Common or evolving fluid and metal sources through time: Lithos, v. 233, p. 2–26, https://doi.org/10.1016/j.lithos.2015.07.011.

Goldfarb, R.J., and Santosh, M., 2014, The dilemma of the Jiaodong gold deposits: Are they unique?: Geoscience Frontiers, v. 5, p. 139–153, https://doi.org/10.1016/j.gsf.2013.11.001.

Griffin, W.L., O'Reilly, S.Y., Afonso, J.C., and Begg, G.C., 2009, The composition and evolution of lithospheric mantle: A re-evaluation and its tectonic implications: Journal of Petrology, v. 50, p. 1185–1204, https://doi.org/10.1093/petrology/egn033.

Griffin, W.L., Begg, G.C., and O'Reilly, S.Y., 2013, Continental-root control on the genesis of magmatic ore deposits: Nature Geoscience, v. 6, p. 905–910, https://doi.org/10.1038/ngeo1954.

Grondahl, C., and Zajacz, Z., 2017, Magmatic controls on the genesis of porphyry Cu-Mo-Au deposits: The Bingham Canyon example: Earth and Planetary Science Letters, v. 480, Supplement C, p. 53–65.

Hronsky, J.M.A., Groves, D.I., Loucks, R.R., and Begg, G.C., 2012, A unified model for gold mineralisation in accretionary orogens and implications for regional-scale exploration targeting methods: Mineralium Deposita, v. 47, p. 339–358, https://doi.org/10.1007/s00126-012-0402-y.

Huang, F., Xu, J.-F., Liu, Y.-S., Li, J., Chen, J.-L., and Li, X.-Y., 2017, Re-Os isotope evidence from Mesozoic and Cenozoic basalts for secular evolution of the mantle beneath the North China craton: Contributions to Mineralogy and Petrology, v. 172, p. 28, https://doi.org/10.1007/s00410-017-1342-4.

Jenner, F.E., and O'Neill, H.S.C., 2012, Analysis of 60 elements in 616 ocean floor basaltic glasses: Geochemistry Geophysics Geosystems, v. 13, Q02005, https://doi.org/10.01029/02011GC004009.

Li, J.-W., Bi, S.-J., Selby, D., Chen, L., Vasconcelos, P., Thiede, D., Zhou, M.-F., Zhao, X.-F., Li, Z.-K., and Qiu, H.-N., 2012, Giant Mesozoic gold provinces related to the destruction of the North China craton: Earth and Planetary Science Letters, v. 349–350, p. 26–37, https://doi.org/10.1016/j.epsl.2012.06.058.

Liu, J., Rudnick, R.L., Walker, R.J., Gao, S., Wu, F.-y., Piccoli, P.M., Yuan, H., Xu, W.-l., and Xu, Y.-G., 2011, Mapping lithospheric boundaries using Os isotopes of mantle xenoliths: An example from the North China craton: Geochimica et Cosmochimica Acta, v. 75, p. 3881–3902, https://doi.org/10.1016/j.gca.2011.04.018.

Liu, Y., Gao, S., Kelemen, P.B., and Xu, W., 2008, Recycled crust controls contrasting source compositions of Mesozoic and Cenozoic basalts in the North China craton: Geochimica et Cosmochimica Acta, v. 72, p. 2349–2376, https://doi.org/10.1016/j.gca.2008.02.018.

Lorand, J.P., Luguet, A., and Alard, O., 2013, Platinum-group element systematics and petrogenetic processing of the continental upper mantle: A review: Lithos, v. 164–167, p. 2–21, https://doi.org/10.1016/j.lithos.2012.08.017.

Maier, W.D., Peltonen, P., McDonald, I., Barnes, S.J., Barnes, S.-J., Hatton, C., and Viljoen, F., 2012, The concentration of platinum-group elements and gold in southern African and Karelian kimberlite-hosted mantle xenoliths: Implications for the noble metal content of the Earth's mantle: Chemical Geology, v. 302, p. 119–135, https://doi.org/10.1016/j.chemgeo.2011.06.014.

Mao, J., Wang, Y., Li, H., Pirajno, F., Zhang, C., and Wang, R., 2008, The relationship of mantle-derived fluids to gold metallogenesis in the Jiaodong Peninsula: Evidence from D-O-C-S isotope systematics: Ore Geology Reviews, v. 33, p. 361–381, https://doi.org/10.1016/j.oregeorev.2007.01.003.

McDonough, W.F., and Sun, S.S., 1995, The composition of the Earth: Chemical Geology, v. 120, p. 223–253, https://doi.org/10.1016/0009-2541(94)00140-4.

McInnes, B.I.A., McBride, J.S., Evans, N.J., Lambert, D.D., and Andrew, A.S., 1999, Osmium isotope constraints on ore metal recycling in subduction zones: Science, v. 286, p. 512–516, https://doi.org/10.1126/science.286.5439.512.

Meng, F., Gao, S., Niu, Y., Liu, Y., and Wang, X., 2015, Mesozoic–Cenozoic mantle evolution beneath the North China craton: A new perspective from Hf-Nd isotopes of basalts: Gondwana Research, v. 27, p. 1574–1585, https://doi.org/10.1016/j.gr.2014.01.014.

Muntean, J.L., Cline, J.S., Simon, A.C., and Longo, A.A., 2011, Magmatic-hydrothermal origin of Nevada's Carlin-type gold deposits: Nature Geoscience, v. 4, p. 122–127, https://doi.org/10.1038/ngeo1064.

O'Reilly, S., and Griffin, W.L., 2013, Mantle metasomatism, in Harlov, D., and Austrheim, H., eds., Metasomatism and the Chemical Transformation of Rock: Berlin, Springer, p. 471–533, https://doi.org/10.1007/978-3-642-28394-9_12.

Pokrovski, G.S., Borisova, A.Y., and Bychkov, A.Y., 2013, Speciation and transport of metals and metalloids in geological vapors: Reviews in Mineralogy and Geochemistry, v. 76, p. 165–218, https://doi.org/10.2138/rmg.2013.76.6.

Saunders, E., Pearson, N.J., O'Reilly, S.Y., and Griffin, W.L., 2018, Gold in the mantle: A global assessment of abundance and redistribution processes: Lithos, v. 322, p. 376–391, https://doi.org/10.1016/j.lithos.2018.10.022.

Tan, J., Wei, J., He, H., Su, F., Li, Y., Fu, L., Zhao, S., Xiao, G., Zhang, F., Xu, J., Liu, Y., Stuart, F.M., and Zhu, R., 2018, Noble gases in pyrites from the Guocheng-Liaoshang gold belt in the Jiaodong Province: Evidence for a mantle source of gold: Chemical Geology, v. 480, p. 105–115, https://doi.org/10.1016/j.chemgeo.2017.09.027.

Tassara, S., González-Jiménez, J.M., Reich, M., Schilling, M.E., Morata, D., Begg, G., Saunders, E., Griffin, W.L., O'Reilly, S.Y., Grégoire, M., Barra, F., and Corgne, A., 2017, Plume-subduction interaction forms large auriferous provinces: Nature Communications, v. 8, p. 843, https://doi.org/10.1038/s41467-017-00821-z.

Wang, Z., Becker, H., and Gawronski, T., 2013, Partial re-equilibration of highly siderophile elements and the chalcogens in the mantle: A case study on the Baldissero and Balmuccia peridotite massifs (Ivrea zone, Italian Alps): Geochimica et Cosmochimica Acta, v. 108, p. 21–44, https://doi.org/10.1016/j.gca.2013.01.021.

Wu, F.-Y., Yagn, J.-H., Xu, Y.-g., Wilde, S.A., and Walker, R.J., 2019, Destruction of the North China craton in the Mesozoic: Annual Review of Earth and Planetary Sciences, v. 47, p. 173–195, https://doi.org/10.1146/annurev-earth-053018-060342.

Xia, Q.-K., Liu, J., Liu, S.-C., Kovács, I., Feng, M., and Dang, L., 2013, High water content in Mesozoic primitive basalts of the North China craton and implications on the destruction of cratonic mantle lithosphere: Earth and Planetary Science Letters, v. 361, p. 85–97, https://doi.org/10.1016/j.epsl.2012.11.024.

Xia, Q.-K., Liu, J., Kovács, I., Hao, Y.-T., Li, P., Yang, X.-Z., Chen, H., and Sheng, Y.-M., 2017, Water in the upper mantle and deep crust of eastern China: Concentration, distribution and implications: National Science Review, v. 6, p. 125–144, https://doi.org/10.1093/nsr/nwx016.

Zhang, H.-F., Sun, M., Zhou, X.-H., Fan, W.-M., Zhai, M.-G., and Yin, J.-F., 2002, Mesozoic lithosphere destruction beneath the North China craton: Evidence from major-, trace-element and Sr-Nd-Pb isotope studies of Fangcheng basalts: Contributions to Mineralogy and Petrology, v. 144, p. 241–254, https://doi.org/10.1007/s00410-002-0395-0.

Zhang, H.-F., Goldstein, S.L., Zhou, X.-H., Sun, M., Zheng, J.-P., and Cai, Y., 2008, Evolution of subcontinental lithospheric mantle beneath eastern China: Re-Os isotopic evidence from mantle xenoliths in Paleozoic kimberlites and Mesozoic basalts: Contributions to Mineralogy and Petrology, v. 155, p. 271–293, https://doi.org/10.1007/s00410-007-0241-5.

Zhao, T., Zhu, G., Lin, S., and Wang, H., 2016, Indentation-induced tearing of a subducting continent: Evidence from the Tan-Lu fault zone, East China: Earth-Science Reviews, v. 152, p. 14–36, https://doi.org/10.1016/j.earscirev.2015.11.003.

Zheng, J., Sun, M., Zhou, M.-F., and Robinson, P., 2005, Trace elemental and PGE geochemical constraints of Mesozoic and Cenozoic peridotitic xenoliths on lithospheric evolution of the North China craton: Geochimica et Cosmochimica Acta, v. 69, p. 3401–3418, https://doi.org/10.1016/j.gca.2005.03.020.

Zhu, R., Xu, Y., Zhu, G., Zhang, H., Xia, Q., and Zheng, T., 2012, Destruction of the North China craton: Science China–Earth Sciences, v. 55, p. 1565–1587, https://doi.org/10.1007/s11430-012-4516-y.

Zhu, R., Fan, H., Li, J., Meng, Q., Li, S., and Zeng, Q., 2015, Decratonic gold deposits: Science China–Earth Sciences, v. 58, p. 1523–1537, https://doi.org/10.1007/s11430-015-5139-x.